

The influence of poly(ethylene oxide) grafting via siloxane tethers on protein adsorption

Ranjini Murthy, Courtney E. Shell, Melissa A. Grunlan*

Department of Biomedical Engineering, Texas A&M University, College Station, TX 77843-3120, USA

ARTICLE INFO

Article history:

Received 20 October 2008

Accepted 28 January 2009

Available online 15 February 2009

Keywords:

Polyethylene oxide

Siloxane

Protein adsorption

Surface grafting

ABSTRACT

Amphiphilic PEO–silanes (a–c) having siloxane tethers of varying lengths with the general formula α -(EtO)₃Si–(CH₂)₂–oligodimethylsiloxane_n–*block*–poly(ethylene oxide)₈–OCH₃ [$n = 0$ (a), $n = 4$ (b), and $n = 13$ (c)] were grafted onto silicon wafers and resistance to adsorption of plasma proteins was measured. Distancing the PEO segment from the hydrolyzable triethoxysilane [(EtO)₃Si] grafting group by a oligodimethylsiloxane tether represents a new method of grafting PEO chains to surfaces. Properties of surfaces grafted with a–c were compared to surfaces grafted with a traditional PEO–silane containing a propyl spacer [(EtO)₃Si–(CH₂)₃–poly(ethylene oxide)₈–OCH₃, PEO control]. As the siloxane tether length increased, chain density of PEO–silanes grafted onto oxidized silicon wafers decreased and hydrophobicity of the PEO–silane increased which led to a decrease in surface hydrophilicity. Despite decreased surface hydrophilicity, resistance to the adsorption of bovine serum albumin (BSA) increased in the order: PEO control < a < b ≈ c and to human fibrinogen (HF) increased in the order: PEO control < a < b < c.

Published by Elsevier Ltd.

1. Introduction

Within minutes of exposure to blood, surfaces of implanted biomaterials adsorb plasma proteins which results in platelet adhesion and activation of coagulation pathways leading to thrombosis and compromising device success [1,2]. Thus, it is desirable for blood-contacting materials to inhibit the adsorption of blood proteins. Among the polymeric biomaterials which have desirable bulk properties but inadequately resist adhesion of proteins are silicones (e.g. poly(dimethylsiloxane, PDMS), poly(ethylene terephthalate) (PET), polypropylene (PP) and poly(ethylene (PE)) [3–6]. Their lack of resistance to protein adsorption is attributed to their hydrophobicity as proteins preferentially adsorb onto hydrophobic, non-polar surfaces [7,8]. In contrast, poly(ethylene oxide) (PEO; or poly(ethylene glycol) PEG) is a neutral, hydrophilic polymer with particularly high resistance to protein adhesion [7–10]. The protein-repelling behavior of PEO is attributed to its hydrophilicity [11] as well as its high configurational mobility which leads to a large excluded volume [12,13], steric repulsion [7,8], blockage of underlying adsorption sites [14], and an entropic penalty if protein adhesion was to occur [7,8,10].

PEO has been immobilized onto polymer surfaces via self-assembly [15,16], physisorption [17,18], formation of surface physical interpenetrating networks (SPINs) [19–21] or by covalent grafting [22–24]. Graft chains can provide long-term chemical stability of new surface functionalities without altering bulk properties of the substrate [5,25,26]. Thus, covalent grafting of PEO onto activated surfaces is considered to be the most effective method to prepare stable PEO surfaces [10]. Surfaces of hydrophobic polymers are hydrophilized upon covalent grafting of PEO thereby improving resistance to protein adsorption while maintaining bulk properties. For instance, epoxide and aldehyde end-functionalized PEO chains were covalently grafted onto functionalized PET surfaces [27] and PEO–silanes were grafted onto the surfaces of oxidized silicones [28,29].

Functional silanes (i.e. coupling agents) are typically used for the purpose of covalent grafting to achieve surface modification [30]. Silane coupling agents are generally trialkoxysilanes which undergo stepwise hydrolysis and condensation with a hydroxylated surface. For conventional PEO–silanes, the PEO segment is distanced from the alkoxy silane groups by a short alkane spacer (e.g. propyl for (RO)₃Si–(CH₂)₃–(CH₂CH₂O)_n–OCH₃) [28,31–35]. We have recently reported the preparation of amphiphilic PEO–silanes (a–c) with flexible siloxane tethers of varying lengths having the general formula α -(EtO)₃Si–(CH₂)₂–oligodimethylsiloxane_n–*block*–poly(ethylene oxide)₈–OCH₃ [$n = 0$ (a), $M_n = 749$ g/mol; $n = 4$ (b),

* Corresponding author. Tel.: +1 979 845 2406; fax: +1 979 845 4450.

E-mail address: mgrunlan@tamu.edu (M.A. Grunlan).

$M_n = 1044$ g/mol; and $n = 13$ (c) $M_n = 1710$ g/mol [36]. Thus, the PEO segment is distanced from the trialkoxysilane group [(EtO)₃Si] by an oligodimethylsiloxane tether. These siloxane tethers are highly flexible due to the wide bond angle ($\sim 143^\circ$) and low barrier to linearization (0.3 kcal/mol) of Si–O–Si of dimethylsiloxanes [37,38]. The dynamic flexibility of Si–O–Si produces polymers with extremely low glass transition temperatures (T_g s) (e.g. PDMS, $T_g = -125^\circ\text{C}$).

The aforementioned hydrophobic polymeric biomaterials may be oxidized to form a hydroxylated surface with an air or O₂ plasma treatment [39]. However, oxidized polymeric surfaces, particularly silicones, are physically unstable and reorganize in different environments (e.g. air and water) [40]. Thus, PEO–silanes grafted onto hydroxylated polymer surfaces undergo significant physical reorganization depending on the environment which subsequently alters the surface concentration of PEO [28]. For this present work, we selected oxidized silicon wafer to serve as a model hydroxylated biomaterial surface. Because a silicon wafer is physically stable, the surface concentration of covalently grafted PEO–silanes is conveniently maintained which allows the effect of PEO–silane structure to be evaluated. Thus, amphiphilic PEO–silanes (a–c) were grafted onto oxidized silicon wafers (Fig. 1). A conventional PEO–silane (EtO)₃Si–(CH₂)₃–poly(ethylene oxide)₈–OCH₃ ($M_n = 588$ g/mol) (no siloxane tether but the same PEO length) was grafted onto wafer to serve as the “PEO control.”

2. Materials and methods

2.1. Materials

Silicon wafers (111) were obtained from University Wafers, Inc. (Boston, MA). All solvents were obtained from Sigma–Aldrich (St. Louis, MO) and thoroughly dried over 4 Å molecular sieves prior to use. Sulfuric acid (H₂SO₄) and hydrogen peroxide (H₂O₂) were obtained from Sigma–Aldrich and were used as received. Alexa Fluor 555-dye conjugate of bovine serum albumin (AF-555 BSA; MW = 66 kDa; lyophilized powder; > 96% BSA) and Alexa Fluor 546-dye conjugate of human fibrinogen (AF-546 HF; MW = 340 kDa; lyophilized powder; 95% clottable protein) were purchased from Molecular Probes, Inc. (Eugene, OR) and used as received. PEO–silanes (a–c) and PEO control were synthesized according to the procedures previously reported [36]. Silastic T-2 (silicone elastomer) was obtained from Dow Corning (Midland, MI).

2.2. Grafting PEO–silanes onto oxidized silicon wafers

Silicon wafers (1" × 1") were first ultrasonically cleaned in acetone (10 min) and washed with deionized (DI) water. Next, wafers were placed in a 7:3 (v/v) concentrated H₂SO₄/30% H₂O₂ (Piranha) solution for 30 min, thoroughly washed with DI water and dried under a stream of nitrogen (N₂). The resulting oxidized wafers (Si^{OH}) were then placed in a sealed jar containing the grafting solution comprised of the designated PEO–silane (a–c or PEO control) at a specified concentration in toluene, placed on a rocker table for 12 h, removed and annealed in a vacuum oven (36 mmHg) at 150 °C for 12 h. To remove unbound PEO–silane, the wafers were subjected to sequential soaking (1 h), sonication (3 min), and rinsing with ethanol, the sequence repeated with DI water and lastly dried under a stream of N₂.

Silastic T-2 (silicone elastomer) was applied to a solvent-cleaned microscope slide with a drawdown bar (30 mil) and allowed to cure at RT for over 72 h. The film thickness for cured Silastic T-2 films was ~ 0.6 mm. A silicone-coated slide served as a hydrophobic “silicone control” with well-known high protein adhesion [41,42]. An oxidized wafer (Si^{OH}) served as a hydrophilic control.

2.3. Ellipsometry

Ellipsometry measurements were performed by null ellipsometry using a Nanofilm EP3SE Spectroscopic Imaging Ellipsometer, with an incident angle of 54° and a wavelength of 532 nm in a four-zone compensator mode to minimize errors in surface homogeneity. For grafted surfaces, the thickness values were determined using a three-layer air–(PEO–silane)–silicon model [43]. The index of refraction (n) of PEO control and a–c was assumed to be that of crystalline PEO ($n = 1.450$). Because PEO chains may be slightly hydrated, even under dry conditions, the true value is not precisely known. However, the index of refraction (n) of crystalline PEO is a good estimate commonly employed for ellipsometry measurements of PEO-grafted surfaces [44,45]. The assumed value of $n = 1.450$ for a–c grafted films is reasonable because the index of refraction of dimethylsiloxane tether component is considered

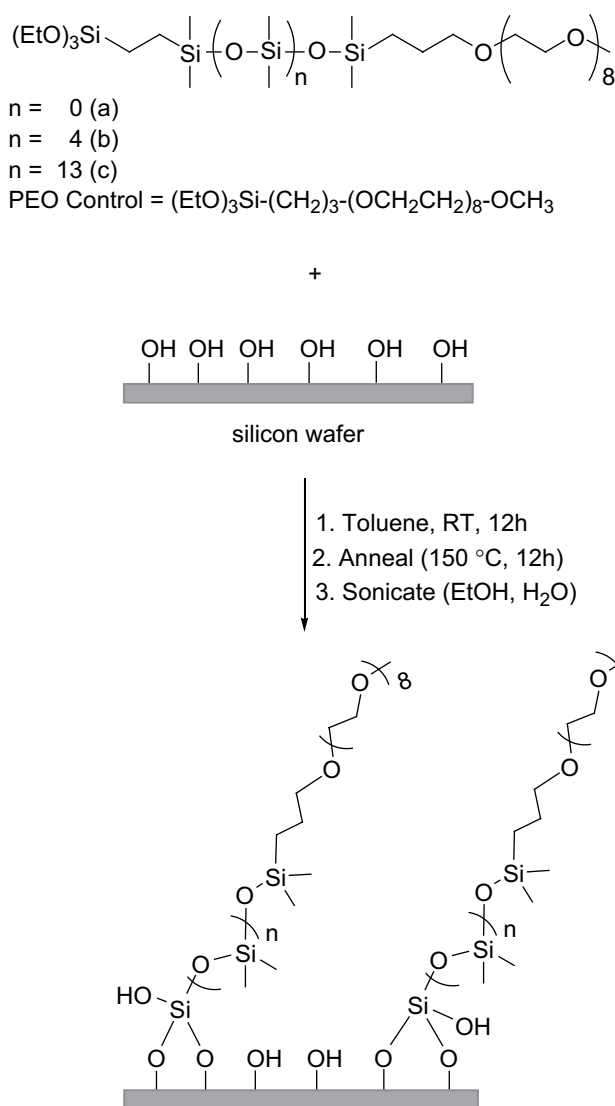


Fig. 1. Grafting of PEO–silanes onto silicon wafer. Oxidized silicon wafers (Si^{OH}) were exposed to toluene-based grafting solutions of a–c and PEO control.

to be that of PDMS ($n = 1.406$) [46,47]. Moreover, it has been shown that variation of 0.05 in the refractive index produces only a 0.1 nm change in thickness [48]. Data was collected in air at a temperature of 20 °C. Thickness values were calculated using the software provided by the manufacturer. From the obtained thickness values, we subtracted the average thickness of the underlying oxide layer to obtain a final thickness (h) of the grafted film (Table 1). The average thickness of the oxide layer was determined by ellipsometry measurements on three different regions of five individual wafers. The obtained average oxide layer thickness of 1.7 ± 0.2 nm is in agreement with literature values [49].

2.4. XPS spectroscopy

Surface composition analysis of PEO–silane grafted silicon wafers was performed using a KRATOS AXIS Ultra Imaging X-ray Photoelectron Spectrometer with a monochromatized Mg K_α source and operating at a base pressure of $\sim 2 \times 10^{-9}$ mbar. The spot size used in all analyses was 7×3 mm. Elemental atomic percent compositions were obtained from survey spectra, which were performed from 0 to 1100 eV. High-resolution analyses with pass energy of 40 eV were performed at a take-off angle of 90°. The binding energies were referenced to C 1s peak at 285.0 eV. The raw data was quantified and analyzed using XPS Peak Processing software.

2.5. Contact angle measurements

Static (θ_{static}), advancing (θ_{adv}), and receding (θ_{rec}) contact angles of distilled/DI water at the surface–air interface were measured at room temperature (RT)

Table 1
Ellipsometry data for grafted surfaces.

Surface (a–c or PEO control)	Grafting solution molarity [mol/L]	Ellipsometry thickness h [nm]	Surface coverage $\Gamma = h \times \rho$ [mg/m ²]	Chain density $\sigma = (6.023I)/M_n$ [chains/nm ²]	Graft distance $D = (4/\pi\sigma)^{1/2}$ [nm]
PEO control	0.0050	3.75 ± 0.7	4.15	4.25	0.55
PEO control	0.0075	4.37 ± 0.4	4.83	4.95	0.51
PEO control	0.0150	3.63 ± 0.1	4.01	4.11	0.56
PEO control	0.0200	3.55 ± 0.2	3.93	4.02	0.56
a	0.0050	1.79 ± 0.2	1.92	1.54	0.91
a	0.0075	2.15 ± 0.3	2.30	1.85	0.83
a	0.0150	3.75 ± 1.0	4.02	3.23	0.63
a	0.0200	2.41 ± 0.4	2.58	2.08	0.78
b	0.0120	2.08 ± 0.3	2.26	1.30	0.99
b	0.0240	3.17 ± 0.3	3.43	1.98	0.80
b	0.0480	3.42 ± 0.2	3.71	2.14	0.77
b	0.0750	4.11 ± 0.2	4.45	2.57	0.70
c	0.0120	3.22 ± 0.3	3.51	1.24	1.02
c	0.0240	3.32 ± 0.5	3.62	1.27	1.00
c	0.0480	4.25 ± 0.3	4.63	1.63	0.88
c	0.0750	3.06 ± 0.5	3.32	1.17	1.04

ρ = density (g/cm³), M_n = number-average molecular weight (g/mol). PEO control = (EtO)₃Si-(CH₂)₃-(OCH₂CH₂)₈-OCH₃ (M_n = 588 g/mol; ρ = 1.16 cm³); a: M_n = 749 g/mol; ρ = 1.07 g/cm³; b: M_n = 1044 g/mol; ρ = 1.08 g/cm³; and c: M_n = 1710 g/mol; ρ = 1.09 g/cm³. Compositions in **boldface** were used in XPS, contact angle analysis and protein studies.

with a CAM-200 (KSV Instruments) contact angle measurement system equipped with an autodispenser, video camera, and drop-shape analysis software. θ_{static} of a sessile drop of water (5 μ L) was measured at 15 sec and 2 min after deposition onto the silicon surface. The θ_{adv} was measured by the addition of 3 μ L (0.25 μ L/sec) of water to a 5 μ L pendant droplet to advance the contact line. θ_{rec} was measured by the subsequent removal of 4 μ L (0.25 μ L/sec) from the same droplet to recede the contact line. The reported θ_{static} , θ_{adv} , and θ_{rec} values are an average of three measurements taken on different areas of the same sample.

2.6. Protein adsorption

Adsorption of bovine serum albumin (AF-555 BSA) and human fibrinogen (AF-546 HF) onto grafted surfaces was evaluated using a Zeiss Axiovert 200 optical microscope equipped with a A-Plan 5 \times objective, AxioCam (HRC Rev. 2), and filter cube (excitation filter of 546 \pm 12 nm [band pass] and emission filter 575–640 nm [band pass]) to obtain fluorescent images on 3 randomly selected regions of the surface. A silicone isolator (20 mm well diameter, 2.5 mm well depth; JTR Press-to-Seal Silicone Isolators) was affixed with adhesive to prevent leakage of solutions from the well. Immediately prior to protein deposition, the wafers were thoroughly washed with phosphate buffered saline (PBS, pH = 7.4) and dried under a stream of N₂. The exposed surface inside each isolator well was filled with 1 mL of AF-555 BSA solution (0.1 mg/mL in PBS) or 1 mL of AF-546 HF solution (0.1 mg/mL in PBS), equilibrated in the dark at RT for 3 h, and removed. One milliliter of fresh PBS was then added to each well and removed after 5 min; this process was repeated for a total of three times. The samples were then dried under a stream of N₂ and imaged. For all samples, the reported protein adsorption value is an average of three measurements taken from different areas of the same sample.

The fluorescent light source was permitted to warm up for 30 min prior to image capture. Linear operation of the camera was ensured and constant exposure time used during the image collection to permit quantitative analyses of the observed fluorescent signals. The fluorescence microscopy images were analyzed using the histogram function of PhotoShop, which yielded the mean and standard deviation of the fluorescence intensity of the whole image. The fluorescence intensity of each AF-555 BSA and AF-546 HF exposed region was subtracted from that of non-exposed region to ensure correction for any fluorescence signal from the material itself. The background-corrected fluorescence intensities for each film were then used to quantify AF-555 BSA and AF-546 HF levels adsorbed by comparison against a calibration curve constructed from the measured fluorescence intensities of AF-555 BSA and AF-546 HF standard samples. The obtained value was converted to mg/cm² by dividing the area inside silicone isolator. Standard samples were prepared by fitting a silicone isolator to unmodified solvent-cleaned silicon wafers (not oxidized) and adding 1 mL of AF-555 BSA or 1 mL of AF-546 HF solutions of known concentrations (0, 0.005, 0.01, 0.02, 0.04 mg/mL AF-555 BSA or AF-546 HF in PBS) to individual wells.

3. Results and discussion

3.1. Ellipsometry

PEO–silanes were grafted with different molar concentrations of grafting solutions. Several parameters were evaluated to characterize the grafted surfaces. The dry thickness of the graft layer (h) was used to estimate the chain density (σ) of PEO–silanes on the surface according to Refs. [10,50–52]:

$$\sigma = \frac{h\rho N_A}{M_n}$$

where h is the grafted layer thickness measured by ellipsometry, ρ is the density of the dry grafted layer (i.e. the density of the PEO–silane), N_A is Avogadro's number and M_n is the number-average molecular weight of the PEO–silane.

Chain density is known to impart a particular conformation to an end-tethered polymer chain [53,54]. A random coil conformation (mushroom regime) occurs when grafting distance (D) is greater than $2R_f$ (the Flory radius; $D > 2R_f$) and a more extended conformation (brush regime) is observed when $D < 2R_f$ [43]. The distance between grafting sites, D (nm), was calculated using the following equation [51]:

$$D = (4/\pi\sigma)^{1/2}$$

The Flory radius (R_f) for an unperturbed surface-anchored random polymer chain in a good solvent (e.g. PEO in water) can be calculated by the Flory equation [43,53,55]:

$$R_f = aN^{3/5}$$

where N is the degree of polymerization (i.e. number of monomers) and a is the length of one monomer, taken to be 0.35 nm for PEO [56].

For all PEO–silanes (a–c and PEO control), $N = 8$ and $2R_f = 2.44$ nm for the PEO segment. The chain density values (σ) for all surface-grafted layers correspond to those required for the onset of the brush regime (i.e. $D < 2R_f$) (Table 1). All chain densities are lower than the estimated upper limit of 5.8 chains/nm² for fully extended PEO chains [43,57].

For a given PEO–silane, increased grafting solution concentration generally produced increased chain density (σ) in the order: $c < b < a < \text{PEO control}$. However, the magnitude of this increase diminished as the siloxane tether length increased (Table 1). Thus, higher chain densities (σ) were obtained with the PEO control and a at lower grafting solution concentrations (0.005–0.02 M) than for b and c at higher grafting solution concentrations (0.012–0.075 M). To obtain surfaces with thickness values (h) similar to PEO control and a grafted surfaces, a minimum grafting solution concentration of 0.0120 M was required for grafting of b and c (Table 1).

The observed dependence of chain density (σ) on grafting solution concentration may be attributed to the M_n of the PEO–silane as well as its solubility in the grafting solvent (toluene). The observed decrease in chain density (σ) with increased M_n of PEO–silanes is attributed to the ability of higher molecular weight chains to more effectively block grafting of subsequent chains. In other words, already grafted longer chains present a greater steric barrier to inhibit further grafting [43,58]. Similarly, it has been observed that PEO chains which are in poor solubility conditions graft at higher chain densities due to their collapsed structure in the grafting solvent [59]. In this study, the solubility of the PEO–silanes increases with increased siloxane tether length since toluene is a good solvent for dimethylsiloxane tether but a poor solvent for the PEO segment. Hence, a and PEO control are less soluble and are more collapsed than b and c which results in a somewhat higher chain density for the former.

A series of PEO–silane grafted surfaces with similar thickness (h) and surface coverage (Γ) values were used to evaluate surface properties and protein adsorption (Table 1, compositions selected for XPS, contact angle analysis and protein studies in boldface). For these selected grafted surfaces, the PEO segments of all of the grafted chains (a–c and PEO control) were determined to be in the brush regime [$D < 2R_f$ (where $2R_f = 2.44$ nm)] and all chain densities are lower than the estimated upper limit of 5.8 chains/nm² for fully extended PEO chains. Thus, although chain density (σ) decreases somewhat with siloxane tether length, comparison of these grafted surfaces with similar h and Γ values and having brush conformations should provide insight into the effect of siloxane tether length on surface properties and resistance to protein adsorption.

3.2. X-ray photoelectron spectroscopy

XPS was used to confirm successful grafting of PEO–silanes onto silicon wafers. The elemental compositions of these surfaces are reported in Table 2. Carbon present on the surface of unmodified silicon wafer was probably adsorbed contamination from the atmosphere [44,60]. The O 1s and Si 2p peaks correspond to the wafer composition. As expected, following grafting, the Si 2p decreased and the C 1s content increased. The observed C 1s peak was fitted with three Gaussian peaks at binding energies: (i) 284–285 eV corresponding to the C–C in the PEO, (ii) 285.8–286.5 eV corresponding to the C–O in PEO and (iii) 286.9–288.5 eV is likely contamination (Fig. 2). Thus, the increased C–O peak intensity of grafted surfaces versus the unmodified silicon wafer confirmed the presence of PEO.

3.3. Contact angle analysis

θ_{static} , θ_{adv} , and θ_{rec} of DI water droplets on grafted surfaces are reported in Table 3. A crosslinked silicone elastomer served as a hydrophobic control. The θ_{static} and observed θ_{adv} values for the PEO control grafted surface are similar to those of PEO-grafted silicon surfaces reported in the literature [44,61]. For surfaces grafted with PEO–silanes, θ_{static} decreased and surface hydrophilicity increased in the order: c < b < a < PEO control. This trend reflects the increase in chain density (σ) or the surface concentration of PEO which similarly increased in the order: c < b < a < PEO control (Table 1). Also, since the siloxane tether is hydrophobic, an increase in tether length contributed to a decrease in hydrophilicity for b and c grafted surfaces. The observed decrease in θ_{static} (15 sec) versus θ_{static} (2 min) for all grafted surfaces may be attributed to the hydration of the PEO segments.

An oxidized silicon wafer (Si^{0x}) was used as a model hydroxylated biomaterial surface because it is physically stable, unlike silicone elastomer surfaces, for instance, which undergo reorganization in different environments [40]. Thus, the surface concentration of covalently grafted PEO–silanes may be conveniently maintained on silicon surfaces which permits evaluation of the effect of PEO–silane structure (i.e. siloxane tether length).

Table 2
XPS elemental analysis.

Surface	C 1s	C–C	C–O	Contamination	O 1s	Si 2p
	Total	284.0–284.9	285.8–286.5	286.9–288.5		
Wafer	27.6	91.3	8.7		28.2	44.2
PEO control	31.7	54.3	36.3	9.4	36.9	31.4
a ($n=0$)	37.4	51.0	44.4	4.6	29.2	33.4
b ($n=4$)	38.9	67.2	26.6	6.2	27.3	33.8
c ($n=13$)	43.6	73.7	21.0	5.3	26.7	29.7

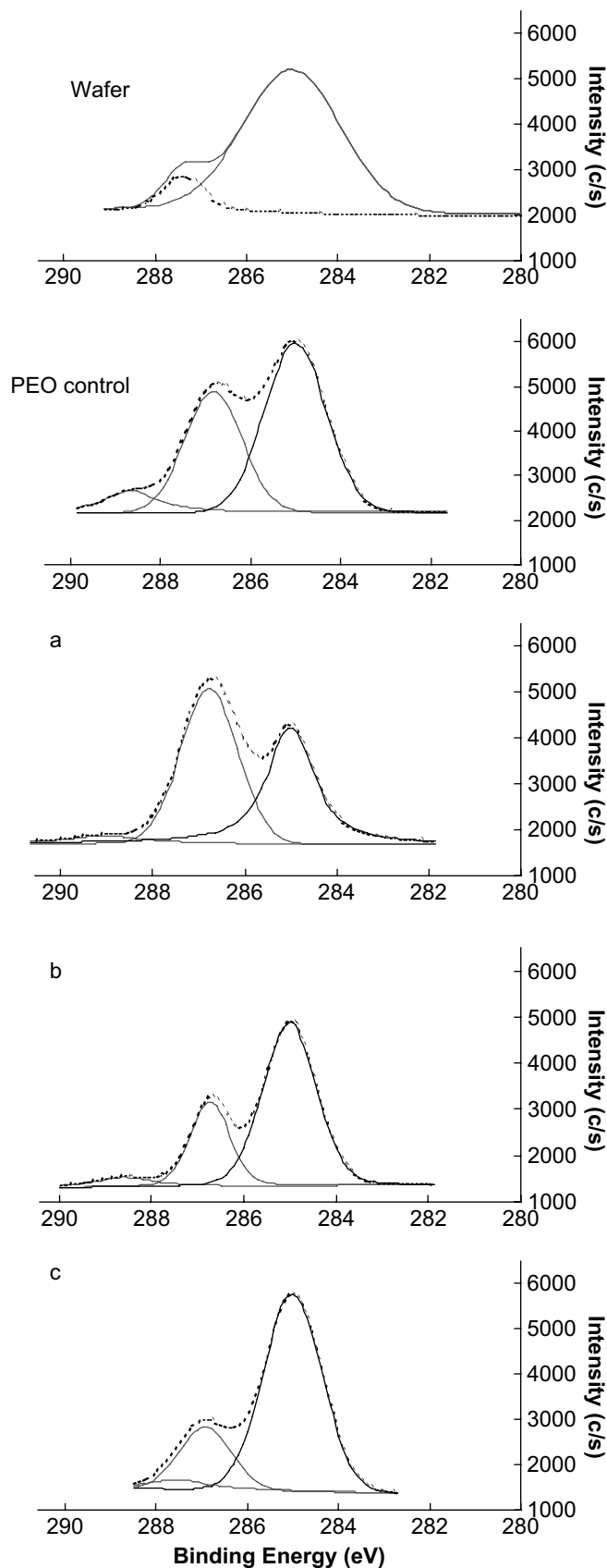


Fig. 2. High-resolution C 1s spectra of unmodified silicon wafer, PEO control and wafers grafted with PEO–silanes (a–c). The increase in C–O is evidence of PEO present at the surface.

Table 3
Contact angle measurements.

Surface grafted with:	Static contact angles		Dynamic contact angles	
	θ_{static} at 15 sec	θ_{static} at 2 min	θ_{adv}	θ_{rec}
Si ^{0x}	21 ± 2.0	16 ± 4.0	24 ± 2.0	23 ± 2.0
PEO control	55 ± 1.0	51 ± 1.0	50 ± 1.0	45 ± 2.0
a (n = 0)	57 ± 1.0	52 ± 0.1	62 ± 0.3	59 ± 1.0
b (n = 4)	79 ± 0.5	75 ± 0.8	85 ± 1.0	83 ± 1.0
c (n = 13)	86 ± 2.0	81 ± 2.0	90 ± 1.0	87 ± 1.0
Silicone	116 ± 1.0	115 ± 1.0	121 ± 1.0	115 ± 1.0

Si^{0x}: oxidized silicon wafer. Silicone = Dow Corning Silastic T-2 cured on a glass microscope slide.

Hysteresis ($\theta_{\Delta} = \theta_{\text{adv}} - \theta_{\text{rec}}$) is typically used as an indicator of surface reorganization [62]. For instance, after a pure silicone surface is wetted, polar Si–O–Si groups reorganize to the film–water interface to minimize interfacial surface tension such that $\theta_{\text{rec}} < \theta_{\text{adv}}$ [40]. Delamarche et al. observed significant hysteresis

(~15°) for surfaces prepared by grafting of (EtO)₃Si–(CH₂)₃–poly(ethylene oxide)₇–OCH₃ onto silicone due to the ability of siloxane and PEO segments to reorganize [28]. The physical stability or absence of surface reorganization of the silicon wafer (Si^{0x}) surface was confirmed by its lack of significant hysteresis. Similarly, PEO–silane grafted surfaces did not exhibit significant hysteresis. In other words, the surface concentration of the grafted PEO–silanes remains constant since the underlying silicon wafer is physically stable. Hence, the observed surface properties may be related to chain density (σ) and the chemical structure of PEO–silanes as stated above.

3.4. Protein adsorption

Albumin is the most abundant plasma protein (60%) and fibrinogen (4%), also a plasma protein, plays an important role in the process of thrombosis as it is converted by thrombin to insoluble fibrin [63]. Thus the amounts of BSA and HF proteins adsorbed

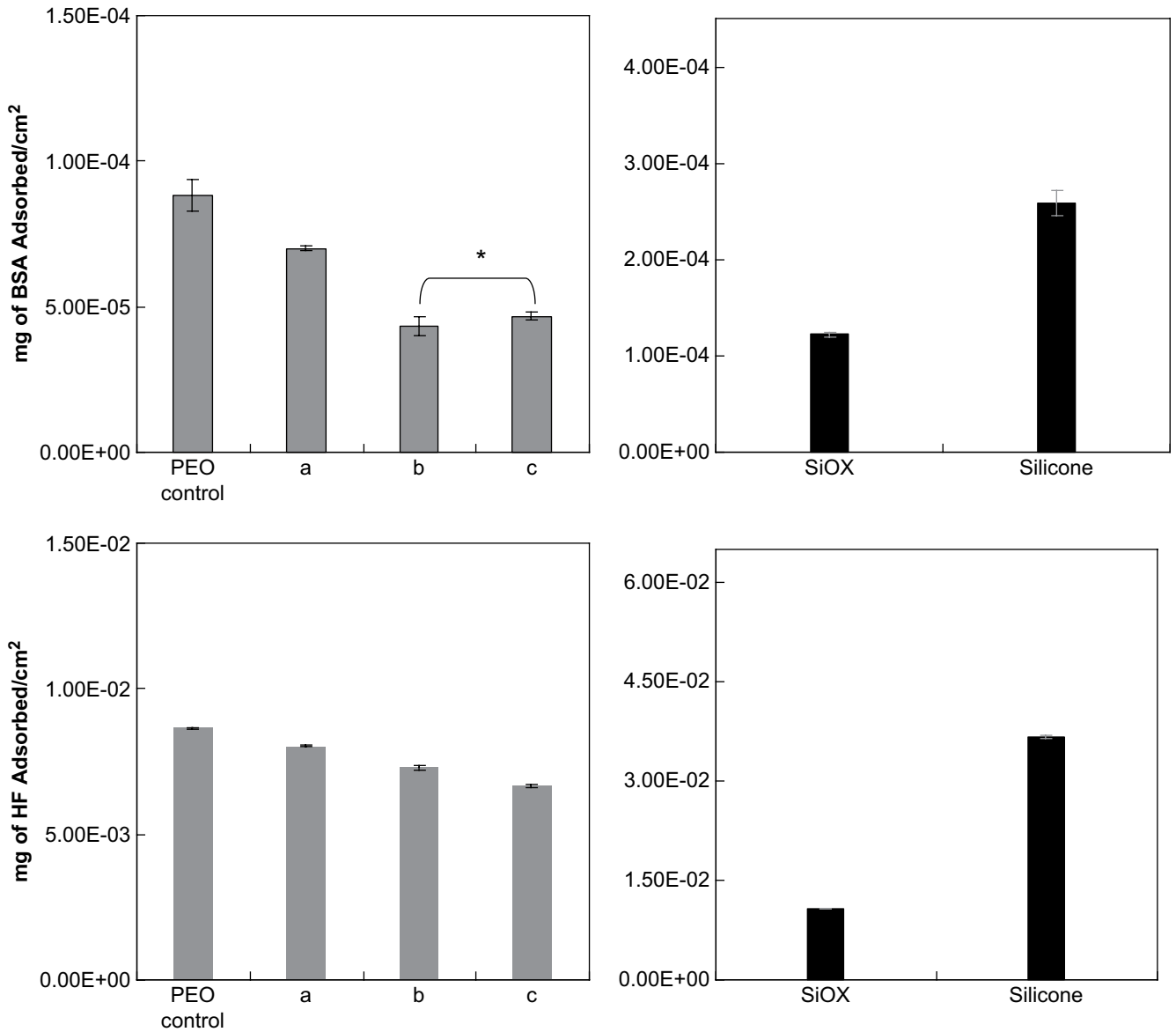


Fig. 3. Adsorption of [Top] BSA and [Bottom] HF onto PEO–silane grafted wafers. Error bars represent the standard deviation between the fluorescence measurements of 3 randomly selected regions. Statistical significance was determined by one-way analysis of variance (Holm–Sidak method where $p = 0.05$ unless otherwise noted. * indicates $p > 0.05$). Si^{0x} = oxidized wafer and Silicone = Dow Corning Silastic T-2 cured on a glass microscope slide.

onto PEO–silane grafted surfaces were analyzed to determine plasma protein adsorption (Fig. 3). Protein adsorption of BSA and HF conjugated with a fluorescent dye was measured via fluorescence microscopy [27,64–66].

As was observed in this study, silicone exhibits high protein adsorption as a result of its extreme hydrophobicity [41,42]. For every surface, higher amounts of HF were adsorbed compared to BSA which is consistent with previous observations [63,67]. The enhanced adhesion of HF compared to BSA is attributed to the former's greater hydrophobicity [68] as well as HF's rod-like geometry which facilitates reorientation on the adsorbing surface to increase protein–protein interaction and surface concentration [63]. The amount of protein adsorbed by grafted surfaces is substantially lower than that adsorbed by the silicone control.

If protein adhesion was controlled by only surface hydrophilicity, one would predict that the PEO control grafted surface would be the most resistant to protein adsorption since it is the most hydrophilic. This trend, however, was not observed. For surfaces grafted with a–c, adsorption of BSA and HF was less compared to a surface grafted with the PEO control. Resistance to BSA adsorption increased with siloxane tether length in the order: PEO control < a < b ≈ c. Adsorption onto b and c grafted surfaces was not statistically different from each other. Similarly, resistance to HF adsorption increased in the order: PEO control < a < b < c. In this case, adsorption onto b and c grafted surfaces was statistically different from each other. Thus, despite the highest surface hydrophobicity due to the lowest chain density (σ) as well as longest hydrophobic siloxane tether, c grafted surfaces exhibited the least protein adsorption. In the absence of surface hydrophilicity to explain the superior protein resistance of surfaces prepared by grafting PEO via longer siloxane tethers, enhanced configurational mobility of the PEO segment may be considered [7,8,12–14]. Although the PEO segments of all of the grafted chains (a–c and PEO control) were determined to be in the brush regime, the chain density (σ) decreased with siloxane tether length. Thus, any enhanced configurational mobility may be attributed not only to the longer siloxane tether, but also to the somewhat lower chain density. Thus, future studies are required to probe the mechanism by which grafting of PEO segments via longer siloxane tethers diminishes protein adsorption. In future studies, we will attempt to prepare silicon surfaces grafted with PEO–silanes (a–c and PEO control) using different solvent and temperature conditions to obtain even more similar chain densities [59]. This would allow us to eliminate any enhanced PEO configurational mobility due to lower chain density and thus examine the contribution of longer siloxane tether towards increased PEO configurational mobility and subsequent enhanced resistance to protein adsorption. In addition to their configurational mobility, the increasing amphiphilic nature of the PEO–silanes (a–c) with longer siloxane tether length may also be considered as a source of their resistance to protein adsorption. Their amphiphilic nature should result in thermodynamically driven phase segregation of the siloxane and PEO segments due to their difference in surface energy. Such phase segregation on surfaces has been previously shown to generate complex surface topographies which resist the adsorption of proteins [69,70].

4. Conclusions

Distancing the PEO segment from the grafting site via a siloxane tether represents a new method of grafting PEO chains to surfaces. PEO–silanes containing siloxane tethers of varying lengths (a–c) were grafted onto the surfaces of oxidized silicon wafers. As the siloxane tether length increased, chain density (σ) decreased due to the greater steric barrier presented by already grafted longer chains

and enhanced solubility of PEO–silanes in the grafting solvent. Surface properties and resistance to protein adsorption were measured using a series of PEO–silane grafted surfaces with similar thickness (h) and surface coverage (Γ) values and in which the PEO segments of all of the grafted PEO–silanes were determined to be in the brush regime and all chain densities were lower than the estimated upper limit of 5.8 chains/nm² for fully extended PEO chains. As a result of decreased chain density (σ) (i.e. decreased PEO surface concentration) and increased length of the hydrophobic siloxane tether, surface hydrophilicity increased in the order: c < b < a < PEO control. However, despite lower chain density (σ) and higher surface hydrophobicity, resistance to BSA adsorption increased in the order of PEO control < a < b ≈ c and resistance to HF adsorption increased in the order of PEO control < a < b < c. In other words, longer siloxane tethers contributed to enhanced resistance to protein adsorption of the PEO–silane. Because hydrophilicity is not enhanced, it is postulated that the improved protein resistance may be due to the enhanced configurational mobility of the PEO segment with a longer siloxane tether as well as the enhanced amphiphilic nature of the PEO–silane. The grafting of amphiphilic PEO–silanes (a–c) onto the surfaces of common polymeric biomaterials may provide enhanced blood-compatibility while maintaining desirable bulk properties.

Acknowledgements

We thank D.E. Bergbreiter (TAMU, Dept. of Chemistry) for use of the CAM-200 contact angle analyzer and Dr. M.S. Hahn (TAMU, Dept. of Chemical Eng.) for guidance with fluorescent microscopy experiments.

References

- [1] Pitt WG, Park K, Cooper SL. Sequential protein adsorption and thrombus deposition on polymeric biomaterials. *J Colloid Interface Sci* 1986;111:343–62.
- [2] Kenausis GL, Vörös J, Elbert DL, Huang N, Hofer R, Ruiz-Taylor L, et al. Poly(L-lysine)-g-poly(ethylene glycol) layers on metal oxide surfaces: attachment mechanism and effect of architecture of resistance of protein adsorption. *J Phys Chem B* 2000;104:3298–309.
- [3] Anderson JM, Ziats NP, Azeez A, Brunstedt MR, Stack S, Bonfield TL. Protein adsorption and macrophage activation on polydimethylsiloxane and silicone rubber. *J Biomater Sci Polym Ed* 1995;7:159–69.
- [4] Park S, Bearinger JP, Lautenschlager EP, Castner DG, Healy KE. Surface modification of poly(ethylene terephthalate) angioplasty balloons with a hydrophilic poly(acrylamide-co-ethylene glycol) interpenetrating polymer network coating. *J Biomed Mater Res* 2000;53:568–76.
- [5] Kato K, Uchida E, Kang E-T, Uyama Y, Ikada Y. Polymer surfaces with graft chains. *Prog Polym Sci* 2003;28:209–59.
- [6] Lee JH, Lee HB. Platelet adhesion onto wettability gradient surfaces in the absence and presence of plasma proteins. *J Biomed Mater Res* 1998;41:304–11.
- [7] Jeon SI, Lee JH, Andrade JD, DeGennes PG. Protein–surface interactions in the presence of polyethylene oxide. *J Colloid Interface Sci* 1991;142:149–58.
- [8] Jeon SI, Andrade JD. Protein–surface interactions in the presence of polyethylene oxide. *J Colloid Interface Sci* 1991;142:159–66.
- [9] Gombotz WR, Guanghui W, Horbett TA, Hoffman AS. Protein adsorption to poly(ethylene oxide) surfaces. *J Biomed Mater Res* 1991;25:1547–62.
- [10] Lee JH, Lee HB, Andrade JD. Blood compatibility of polyethylene oxide surfaces. *Prog Polym Sci* 1995;20:1043–79.
- [11] Elbert DL, Hubbell JA. Surface treatments of polymers for biocompatibility. *Annu Rev Mater Sci* 1996;26:365–94.
- [12] Knoll D, Hermans J. Polymer–protein interactions. *J Biol Chem* 1983;258:5710–5.
- [13] Oesterberg E, Bergstroem K, Holmberg K, Riggs JA, Van Alstine JM, Schuman TP, et al. Comparison of polysaccharide and poly(ethylene glycol) coatings for reduction of protein adsorption on polystyrene surfaces. *Colloids Surf A Physiochem Eng Aspects* 1993;77:159–69.
- [14] McPherson T, Kidane A, Szeifer I, Park K. Prevention of protein adsorption by tethered poly(ethylene oxide) layers: experiments and single-chain mean-field analysis. *Langmuir* 1998;14:176–86.
- [15] Prime KL, Whitesides GM. Adsorption of proteins onto surfaces containing end-attached oligo(ethylene oxide): a model system using self-assembled monolayers. *J Am Chem Soc* 1993;115:10714–21.
- [16] Pale-Grosdemange C, Simon ES, Prime KL, Whitesides GM. Formation of self-assembled monolayers of chemisorption of derivatives of oligo(ethylene glycol) of structure HS(CH₂)_n(OCH₂CH₂)_mOH on gold. *J Am Chem Soc* 1991;113:12–20.

- [17] Huang Y-W, Gupta VK. Influence of polymer flux and chain length on adsorption of poly(ethylene oxide) on physically heterogeneous surfaces. *Langmuir* 2002;18:2280–7.
- [18] Ruiz-Taylor LA, Martin TL, Zaugg FG, Witte K, Indermuhle P, Nock S, et al. Monolayers of derivatized poly(L-lysine)-grafted poly(ethylene glycol) on metal oxides as a class of biomolecular interfaces. *Proc Natl Acad Sci U S A* 2001;3:852–7.
- [19] Desai NP, Hubbell JA. Surface physical interpenetrating polymer networks of poly(ethylene terephthalate) and poly(ethylene oxide) with biomedical applications. *Macromolecules* 1992;25:226–332.
- [20] Desai NP, Hubbell JA. Solution technique to incorporate polyethylene oxide and other water-soluble polymers into surfaces of polymeric biomaterials. *Biomaterials* 1991;12:144–53.
- [21] Ikada Y. Surface modification of polymers for medical applications. *Biomaterials* 1994;15:725–36.
- [22] Gombotz WR, Guanghui W, Hoffman AS. Immobilization of poly(ethylene oxide) on poly(ethylene terephthalate) using a plasma polymerization process. *J Appl Polym Sci* 1989;37:91–107.
- [23] Sofia SJ, Premnath V, Merrill EW. Poly(ethylene oxide) grafted to silicon surfaces: grafting density and protein adsorption. *Macromolecules* 1998;31:5059–70.
- [24] Malmsten M, Emoto K, Van Alstine JM. Effect of chain density on inhibition of protein adsorption by poly(ethylene glycol) based coatings. *J Colloid Interface Sci* 1998;202:507–17.
- [25] Bhattacharya A, Misra BN. Grafting: a versatile means to modify polymers. Techniques, factors, and applications. *Prog Polym Sci* 2004;29:767–814.
- [26] Uyama Y, Kato K, Ikada Y. Surface modification of polymers by grafting. *Adv Polym Sci* 1998;137:3–39.
- [27] Fukai R, Dakwa PHR, Chen W. Strategies toward biocompatible artificial implants: grafting of functionalized poly(ethylene glycols) to poly(ethylene terephthalate) surfaces. *J Polym Sci Part A Polym Chem* 2004;42:5389–400.
- [28] Delamarche E, Donzel C, Kamounah FS, Wolf H, Geissler M, Stutz R, et al. Microcontact printing using poly(dimethylsiloxane) stamps hydrophilized by poly(ethylene oxide) silanes. *Langmuir* 2003;19:8749–58.
- [29] Abbasi F, Mirzadeh H, Katbab A-A. Modification of polysiloxanes for biomedical applications: a review. *Polym Int* 2001;50:1279–87.
- [30] Brook MA. Silicon in organic, organometallic, and polymer chemistry. New York: John Wiley & Sons, Inc.; 2000.
- [31] Sui G, Wang J, Lee C-C, Lu W, Lee SP, Leyton JV, et al. Solution-phase surface modification in intact poly(dimethylsiloxane) microfluidic channels. *Anal Chem* 2006;78:5543–51.
- [32] Papra A, Bernard A, Juncker D, Larsen NB, Michel B, Delamarche E. Microfluidic networks made of poly(dimethylsiloxane), Si, and Au coated with poly(ethylene glycol) for patterning proteins onto surfaces. *Langmuir* 2001;17:4090–5.
- [33] Chen H, Brook MA, Sheardown H. Silicone elastomers for reduced protein adsorption. *Biomaterials* 2004;25:2273–82.
- [34] Chen H, Brook MA, Chen Y, Sheardown H. Surface properties of PEO–silicone composites: reducing protein adsorption. *J Biomater Sci Polym Ed* 2005;16:531–48.
- [35] Chen H, Zhang Z, Chen Y, Brook MA, Sheardown H. Protein repellent silicone surfaces by covalent immobilization of poly(ethylene oxide). *Biomaterials* 2005;26:2391–9.
- [36] Murthy R, Cox CD, Hahn MS, Grunlan MA. Protein-resistant silicones: incorporation of poly(ethylene oxide) via siloxane tethers. *Biomacromolecules* 2007;8:3244–52.
- [37] Mark JE. Silicon-containing polymers. In: Zeigler JM, Fearon FWG, editors. *Silicon-based polymer science: a comprehensive resource. Advances in chemistry series, vol. 224.* Washington, D.C.: American Chemical Society; 1990. p. 47–53.
- [38] Lane TH, Burns SA. Silica, silicon and silicones. Unraveling the mystery. In: Potter M, Rose NR, editors. *Immunology of silicones.* Berlin: Springer; 1996. p. 7.
- [39] Ferguson GS, Chaudhury MK, Biebuyck HA, Whitesides GM. Monolayers in disordered substrates: self-assembly of alkytrichlorosilanes on surface-modified polyethylene and poly(dimethylsiloxanes). *Macromolecules* 1993;26:5870–5.
- [40] Owen MJ, Smith PJ. Plasma treatment of polydimethylsiloxanes. *J Adhes Sci Technol* 1994;8:1063–75.
- [41] Bartzoka V, McDermott MR, Brook MA. Protein–silicone interactions. *Adv Mater* 1999;11:257–9.
- [42] Hron P. Hydrophilisation of silicone rubber for medical applications. *Polym Int* 2003;52:1531–9.
- [43] Unsworth LD, Tun Z, Sheardown H, Brash JL. Chemisorption of thiolated poly(ethylene oxide) to gold: surface chain densities measured by ellipsometry and neutron reflectometry. *J Colloid Interface Sci* 2005;281:112–21.
- [44] Moreau O, Portella C, Massicot F, Henry JM, Riquet AM. Adhesion on poly(ethylene glycol) and quaternary ammonium salt-grafted silicon surfaces: influence of physicochemical properties. *Surf Coat Technol* 2007;201:5994–6004.
- [45] Zhu X-Y, Jun Y, Staarup DR, Major RC, Danielson S, Boaidjiev V, et al. Grafting of high-density poly(ethylene glycol) monolayers on Si(111). *Langmuir* 2001;17:7798–803.
- [46] Vezenov DV, Mayers BT, Wolfe DB, Whitesides GM. Integrated fluorescent light source for optofluidic applications. *Appl Phys Lett* 2005;86:411041–3.
- [47] Branch DW, Wheeler BC, Brewer GJ, Leckband DE. Long-term stability of grafted polyethylene glycol surfaces for use with microsampled substrates in neuronal cell culture. *Biomaterials* 2001;22:1035–47.
- [48] Le Grange JD, Markham SL, Kurkjian CR. Effect of surface hydration on the deposition of silane monolayers on silica. *Langmuir* 1993;9:1749–53.
- [49] Kohli P, Blanchard GJ. Applying polymer chemistry to interfaces: layer-by-layer and spontaneous growth of covalently bound multilayers. *Langmuir* 2000;16:4655–61.
- [50] Sharma S, Johnson RW, Desai TA. Ultrathin poly(ethylene glycol) films for silicon-based microdevices. *Appl Surf Sci* 2003;206:218–29.
- [51] Zdyrko B, Klep V, Luzinov I. Synthesis and surface morphology of high-density poly(ethylene glycol) grafted layers. *Langmuir* 2003;19:10179–87.
- [52] Feng W, Brash JL, Zhu S. Non-biofouling materials prepared by atom transfer radical polymerization grafting of 2-methacryloyloxyethyl phosphorylcholine: separate effects of graft density and chain length on protein repulsion. *Biomaterials* 2006;27:847–55.
- [53] Allen C, Dos Santos N, Gallagher R, Chiu GNC, Shu Y, Li WM, et al. Controlling the physical behavior and biological performance of liposome formulations through use of surface grafted poly(ethylene glycol). *Biosci Reports* 2002;22:225–50.
- [54] Ligoure C, Leibler L. Thermodynamics and kinetics of grafting end-functionalized polymers to an interface. *J Phys* 1990;51:1313–28.
- [55] Soong R, Macdonald PM. PEG molecular weight and lateral diffusion of PEG-ylated lipids in magnetically aligned bicelles. *Biochim Biophys Acta* 2007;1768:1805–14.
- [56] Hristova K, Needham D. Phase behavior of lipid/polymer mixture in aqueous medium. *Macromolecules* 1995;28:991–1002.
- [57] Harder P, Grunze M, Dahint R, Whitesides GM, Laibinis PE. Molecular conformation in oligo(ethylene glycol)-terminated self-assembled monolayers on gold and silver surfaces determines their ability to resist protein adhesion. *J Phys Chem B* 1998;102:426–36.
- [58] Groll J, Ademovic Z, Ameringer T, Klee D, Moeller M. Comparison of coatings from reactive star shaped PEG-*stat*-PPG prepolymers and grafted linear PEG for biological and medical applications. *Biomacromolecules* 2005;6:956–62.
- [59] Wei J, Bagge Ravn D, Gram L, Kingshott P. Stainless steel modified with poly(ethylene glycol) can prevent protein adsorption but not bacterial adhesion. *Colloids Surf B Biointerfaces* 2003;32:275–91.
- [60] Seah MP, Qiu JH, Cumpson PJ, Castle JE. Simple method of depth profiling (stratifying) contamination layers, illustrated by studies on stainless steel. *Surf Interface Anal* 1994;21:336–41.
- [61] Andruzzi L, Senaratne W, Hexemer A, Sheets ED, Ilic B, Kramer EJ, et al. Oligo(ethylene glycol) containing polymer brushes as bioselective surfaces. *Langmuir* 2005;21:2495–504.
- [62] Johnson Jr RE, Dettre RH. Contact angle hysteresis: III. Study of an idealized heterogeneous surface. *J Phys Chem* 1964;68:1744–50.
- [63] Roach P, Farrar D, Perry CC. Interpretation of protein adsorption: surface-induced conformational changes. *J Amer Chem Soc* 2005;127:8168–73.
- [64] Gudipati SC, Finlay JA, Callow JA, Callow ME, Wooley KL. The antifouling and fouling-release performance of hyperbranched fluoropolymer (HBFP)-poly(ethylene glycol) (PEG) composite coatings evaluated by adsorption of biomacromolecules and the green fouling alga *Ulva*. *Langmuir* 2005;21:3044–53.
- [65] Taylor M, Urquhart AJ, Anderson DG, Williams PM, Langer R, Alexander MR, et al. A methodology for investigating protein adhesion and adsorption to microarrayed combinatorial polymers. *Macromol Rapid Commun* 2008;29:1298–302.
- [66] Fujimoto K, Tadokoro H, Ueda Y, Ikada Y. Polyurethane surface modification by graft polymerization of acrylamide for reduced protein adsorption and platelet adhesion. *Biomaterials* 1993;14:442–8.
- [67] Absolom DR, Zingg W, Neumann AW. Protein adsorption to polymer particles: role of surface properties. *J Biomed Mater Res* 1987;21:161–71.
- [68] Lin FYH, Policova Z, Yueh HK, Moy E, Neumann AW. Application of freezing front technique and axisymmetric drop shape analysis-profile for the determination of surface tensions of adsorbed proteins. *Colloids Surf B Biointerfaces* 1993;1:23–32.
- [69] Gudipati SC, Finlay JA, Callow JA, Callow ME, Wooley KL. Hyperbranched fluoropolymer and linear poly(ethylene glycol) based amphiphilic crosslinked networks as efficient antifouling coatings: an insight into the surface compositions, topographies, and morphologies. *J Polym Sci Part A Polym Chem* 2004;42:6193–8207.
- [70] Hester JF, Banerjee P, Won YY, Akthakul A, Acar MH, Mayes A. Preparation of protein-resistance surfaces on poly(vinylidene fluoride) membranes via surface segregation. *Macromolecules* 2000;32:1643–50.